End-Effector Trajectory Tracking in Flexible Arms: Comparison of Approaches Based on Regulation Theory

A. De Luca, L. Lanari, G. Ulivi

Dipartimento di Informatica e Sistemistica
Università degli Studi di Roma "La Sapienza"
Via Eudossiana 18, 00184 Roma, Italy

Abstract

Accurate tracking of end-effector trajectories is one of the most demanding tasks for robot arms with flexible links. This problem is tackled here using regulation theory, considering the nonlinearities of the general dynamic model. The control design is presented in detail, including output trajectory generation, associated reference state computation, and different feedforward/feedback realizations of the regulation concept. Extensive simulations on a simple but representative case study validate the analysis and allow to compare the various approaches.

1. Introduction

Lightweight flexible structures are receiving increasing interest in robotic applications as they require smaller actuators to obtain higher performance, e.g. in terms of motion speed [1]. Typically, the most significative but demanding task to be executed is the tracking of desired trajectories for the robot end-effector. Starting from the experience gained in vibration suppression for large space structures [2], a common control approach is to superimpose active modal damping to standard techniques for controlling the rigid body motion [3,4]. For point-to-point tasks, a clever application of such composed strategies may lead to acceptable results. However, when considering motion along a trajectory, these methods cannot avoid deviations of the arm tip from the nominal path during the slew. On the other hand, use of inversion techniques for exact reproduction of end-effector trajectories induces in general instability in the closed-loop behavior [5]. When the tip position is the controlled output, the system input-output mapping is *non-minimum phase*, a concept defined both in the linear and nonlinear setting [6,7]. As a consequence, direct inversion is unfeasible due to the forced cancellation of unstable zero-dynamics.

For this class of systems, a convenient way to achieve asymptotic output tracking while preserving internal stability is to follow a *regulation* approach. End-effector motion control via nonlinear regulation has been successfully demonstrated in [8,9] for a one-link flexible arm. The rationale of this control scheme goes beyond cancellation of nonlinearities, yet producing quite good tracking results. Suppose to apply in open-loop a bounded input torque at the joint level: the flexible arm, being a passive mechanical device, will display bounded deformations and, accordingly, the end-effector will move

along a certain trajectory. At this stage, no form of instability may ever occurr. If the desired output trajectory coincides with (or is part of) this motion, the robot arm must experience the same deformation history, even under closed-loop control. Therefore, the controller itself has to generate this evolution as a reference for the system state, starting from the specified output trajectory. Moreover, any feedback action should force the internal state of the system towards this 'natural' time-varying deflection, so that the end-effector will eventually move as desired. The regulator control structure is tailored to this qualitative description: an exosystem generates both the desired output trajectory and the associated state evolution, while a stabilizing linear feedback guarantees attractivity of this state-space reference trajectory.

The initial conditions of the arm play an important role in understanding the type of end-effector tracking behavior (exact vs. asymptotic) with respect to an arbitrary motion. If the full state is assigned at the initial time, i.e. when the trajectory starts, and does not match the necessary one, then a transient output error will exist, although the stabilizing action of the regulator will let it decay to zero. On the other hand, when input torques are allowed to be applied to the system also ahead of time, it is possible to bring the flexible arm into the proper deformation state at the initial time. From there on, the desired trajectory will be exactly reproduced at the system output. This interpretation points out the relations with other strategies, sometimes referred as *non-causal* solutions to the inversion problem, which are typical of frequency domain approaches [10] and of iterative learning schemes [11]. Off-line optimal control laws also yield similar input profiles [12].

In [8], nonlinear regulation theory was applied for the first time to the tracking of sinusoidal end-effector motions of a flexible arm. Some viable alternatives in the regulator design have been presented in [9]. Taking advantage of a preliminary input-output inversion control law, regulation can be performed using several combinations of feedforward/feedback terms. In particular, *direct*, *indirect* and *mixed* designs were introduced, including different amounts of nonlinear state feedback. For illustration purposes, developments in [8,9] were carried out for a one-link flexible arm, using a simple nonlinear dynamic model with flexibility concentrated in an elastic spring located along the link.

In this paper, the regulator approach is further investigated for the common nonlinear model of flexible robotic arms, thus including also the multi-link case, with the aim of tracking general end-effector trajectories. Further insights are provided into the actual computation of the controller terms, showing in particular some properties of an efficient approximation technique. Next, the single steps involved in the regulator synthesis will be outlined using the same one-link flexible arm as in [8,9]. In this case study, the direct, indirect and mixed nonlinear regulator designs are compared in terms of practical tracking performance. Reference trajectories are chosen so to obtain smooth interpolated motions. With this respect, cubic and fifth-order polynomials are tested by simulation and numerical results indicate that very limited transient errors can be obtained, even when starting the arm from the standard rest condition. For completeness, also tracking results obtained with a linear regulator are given. The reported analysis provides the basis for dealing with more complex robotic applications, well beyond the case study presented here.

2. Nonlinear Regulation of Flexible Robot Arms

The results on output tracking via nonlinear regulation using static state feedback are briefly recalled, referring to the seminal paper [13] for details and technical assumptions. Alternate design procedures are presented for the class of nonlinear invertible systems. These theoretical findings are then reformulated for a general dynamic model of flexible robot arms, illustrating the main computational steps involved and their significance.

2.1 Output Regulation of Nonlinear Systems

Consider an n-dimensional nonlinear system

$$\dot{\mathbf{x}} = \mathbf{f}(\mathbf{x}) + \mathbf{g}(\mathbf{x})\mathbf{u}, \qquad \mathbf{y} = \mathbf{h}(\mathbf{x}), \tag{1}$$

with m inputs and outputs, and assume that its linear approximation at $\mathbf{x} = \mathbf{0}$ is stabilizable by means of a linear state feedback $\mathbf{u} = \mathbf{F}\mathbf{x}$. A reference trajectory $\mathbf{y}_d(t)$ is supposed to be generated by an autonomous r-dimensional dynamic system (i.e. an *exosystem*)

$$\dot{\mathbf{w}} = \mathbf{s}(\mathbf{w}), \qquad \mathbf{y}_d = \mathbf{q}(\mathbf{w}). \tag{2}$$

Vector functions $\mathbf{f}$ and $\mathbf{h}$ are assumed to be zero at $\mathbf{x} = \mathbf{0}$, as well as $\mathbf{s}$ and $\mathbf{q}$ at $\mathbf{w} = \mathbf{0}$. Although the control design is carried out for a fixed exosystem, note that a whole class of trajectories can be generated by varying the initial conditions $\mathbf{w}(0)$.

The problem of tracking a sufficiently well behaved reference trajectory $\mathbf{y}_d(t)$ on a limited time horizon, while preserving stability in the closed-loop system, can be solved finding a state feedback law of the form

$$\mathbf{u} = \gamma(\mathbf{w}) + \mathbf{F}(\mathbf{x} - \pi(\mathbf{w})), \tag{3}$$

where the smooth vector functions $\gamma(\mathbf{w})$ and $\pi(\mathbf{w})$ are zero at $\mathbf{w} = \mathbf{0}$ and satisfy the following equations:

$$\frac{\partial \pi}{\partial \mathbf{w}}\mathbf{s}(\mathbf{w}) = \mathbf{f}(\pi(\mathbf{w})) + \mathbf{g}(\pi(\mathbf{w}))\gamma(\mathbf{w}), \tag{4a}$$

$$\mathbf{q}(\mathbf{w}) = \mathbf{h}(\pi(\mathbf{w})). \tag{4b}$$

The mapping $\pi(\mathbf{w})$ characterizes the desired state evolution associated to the output trajectory $\mathbf{y}_d$, and thus it will also be denoted as $\mathbf{x}_d$. The feedforward action $\gamma(\mathbf{w})$ in the regulator law (3) is needed to keep the state evolving in time exactly as $\mathbf{x}_d(t)$, once an initial state error has been reduced to zero. The linear feedback action (i.e. $\mathbf{F}$) guarantees this attraction to $\mathbf{x}_d$, at least locally.

The set of n partial differential equations (4a) implicitly constrains the search for $\pi(\mathbf{w})$ to actual trajectories of the forced system. The m algebraic relations (4b) simply express the fact that the output behaves as desired, or $\mathbf{y} = \mathbf{y}_d$, when the state is the required one. In particular, if the initial state matches the desired one, $\mathbf{x}(0) = \mathbf{x}_d(0) = \pi(\mathbf{w}(0))$, then exact output reproduction will result. Otherwise, only asymptotic tracking is obtained. Moreover, boundedness of the exosystem state $\mathbf{w}$, and thus of the desired output trajectory $\mathbf{y}_d$, implies in general that of the solution $\pi(\mathbf{w})$ to (4), i.e. of the state trajectory $\mathbf{x}_d$. Note that, if a suitable approximation $\widehat{\pi}(\mathbf{w})$ to

$\pi(\mathbf{w})$ is used in the regulator realization, the closed-loop stability will still be guaranteed while the resulting output error is easily computed as $\mathbf{y}_d(t) - \mathbf{h}(\widehat{\pi}(\mathbf{w}(t)))$.

The overall block diagram of this *direct* nonlinear regulator is reported in Fig. 1. The term 'nonlinear' refers here to the nature of the controlled system (1), implying that both $\pi(\mathbf{w})$ and $\gamma(\mathbf{w})$ are in general nonlinear functions of the exosystem state.

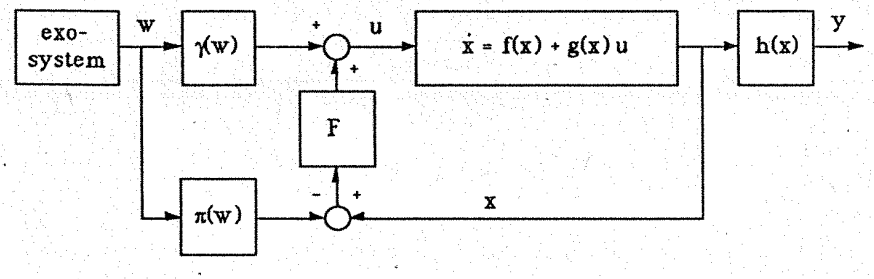

Fig. 1 – Nonlinear regulator: direct design

Indeed, replacing the system model (1) with a linear one

$$\mathbf{f}(\mathbf{x}) = \mathbf{A}\mathbf{x}, \qquad \mathbf{g}(\mathbf{x}) = \mathbf{B}, \qquad \mathbf{h}(\mathbf{x}) = \mathbf{H}\mathbf{x}, \tag{5}$$

and using a linear exosystem

$$\mathbf{s}(\mathbf{w}) = \mathbf{S}\mathbf{w}, \qquad \mathbf{q}(\mathbf{w}) = \mathbf{Q}\mathbf{w}, \tag{6}$$

yields linear forms $\pi(\mathbf{w}) = \Pi\mathbf{w}$, $\gamma(\mathbf{w}) = \Gamma\mathbf{w}$ as solutions of (4), which in turn collapse into the standard matrix equations

$$\Pi\mathbf{S} = \mathbf{A}\Pi + \mathbf{B}\Gamma, \tag{7a}$$

$$\mathbf{Q} = \mathbf{H}\Pi. \tag{7b}$$

The resulting linear regulator is

$$\mathbf{u} = \Gamma\mathbf{w} + \mathbf{F}(\mathbf{x} - \Pi\mathbf{w}). \tag{8}$$

Note that (5) could represent the linear approximation of (1) at $\mathbf{x} = \mathbf{0}$.

In [8], two other schemes that realize the same nonlinear regulation concept were introduced, assuming that system (1) is invertible [14]. In the case of a flexible robot arm, it is known [5] that input-output inversion can be achieved by means of a purely static state feedback of the form

$$\mathbf{u} = \alpha(\mathbf{x}) + \beta(\mathbf{x})\mathbf{v}, \qquad \text{with } \beta(\mathbf{x}) \text{ nonsingular.} \tag{9}$$

When this nonlinear feedback is applied, a proper change of coordinates $\widetilde{\mathbf{x}} = \Psi(\mathbf{x})$ will display the linearity in the resulting input-output behavior. The state-space trasformation may equivalently be performed before using (9). Completing a direct synthesis of

the regulator on the new input $\mathbf{v}$, the input fed into the original plant will be a truly nonlinear state feedback control law,

$$\mathbf{u} = \alpha(\mathbf{x}) + \beta(\mathbf{x})\left[\tilde{\gamma}(\mathbf{w}) + \tilde{\mathbf{F}}(\tilde{\mathbf{x}} - \tilde{\pi}(\mathbf{w}))\right], \tag{10}$$

where a tilda denotes quantities computed after the application of the inversion law (9). The overall *indirect* regulator is shown in Fig. 2.

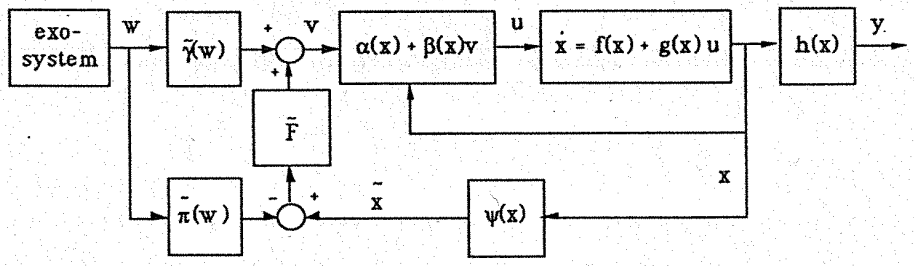

Fig. 2 – Nonlinear regulator: indirect design

In this two-stage approach, inversion control typically cancels 'hard' nonlinearities present in the original system, based on the *measured* state. The composition of (1) with (9) may result in an unstable closed-loop system, which however inherits the original stabilizability property. Thus, the following regulation stage will mainly take care of instabilities.

A third regulation scheme is obtained by computing nonlinear terms in (9) along the nominal state trajectory $\pi(\mathbf{w})$, instead of at the current state $\mathbf{x}$. The control input becomes

$$\mathbf{u} = \alpha(\pi(\mathbf{w})) + \beta(\pi(\mathbf{w}))\big(\tilde{\gamma}(\mathbf{w}) + \mathbf{F}(\mathbf{x} - \pi(\mathbf{w}))\big), \tag{11}$$

and the resulting block diagram of this *mixed* design is shown in Fig. 3. Here, stabilization (e.g. through pole placement) is obtained using a time-varying matrix $\beta(\pi(\mathbf{w}))\mathbf{F}$. This gain modulation is expected to give better results than the constant linear feedback of the direct design. Note also that any combination of measured or nominal states could be used in evaluating single components within α or β.

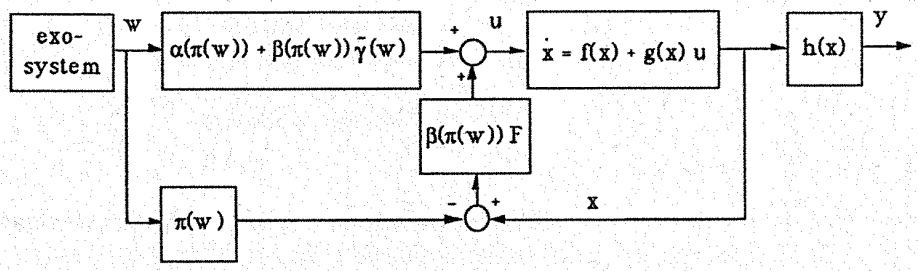

Fig. 3 – Nonlinear regulator: mixed design

2.2 End-Effector Regulation of Flexible Robot Arms

In the following, the regulator equations (4) will be specified for the set of second-order nonlinear differential equations, describing a controlled mechanical system. In particular, consider a robot arm with an open kinematic chain structure, rotational joints and flexible links. The dynamic model is of the form

$$\begin{bmatrix} \mathbf{B}_{11}(\theta,\delta) & \mathbf{B}_{12}(\theta,\delta) \\ \mathbf{B}_{12}^{\mathrm{T}}(\theta,\delta) & \mathbf{B}_{22}(\theta,\delta) \end{bmatrix} \begin{bmatrix} \ddot{\theta} \\ \ddot{\delta} \end{bmatrix} + \begin{bmatrix} \mathbf{n}_1(\theta,\delta,\dot{\theta},\dot{\delta}) \\ \mathbf{n}_2(\theta,\delta,\dot{\theta},\dot{\delta}) \end{bmatrix} + \begin{bmatrix} \mathbf{0} \\ \mathbf{K}\delta \end{bmatrix} + \begin{bmatrix} \mathbf{D}_1\dot{\theta} \\ \mathbf{D}_2\dot{\delta} \end{bmatrix} = \begin{bmatrix} \mathbf{u} \\ \mathbf{0} \end{bmatrix}, \qquad (12)$$

where θ are the N rigid joint variables, and δ are the N_e generalized coordinates associated to deformations. $\mathbf{B}_{ij}$ are blocks of the positive definite inertia matrix, partitioned according to the rigid and flexible components. Similarly, $\mathbf{n}_i$ contain the Coriolis, centrifugal and gravity terms. The diagonal matrix $\mathbf{D}_1$ represents joint viscous friction, while the positive definite, symmetric (and typically diagonal) matrices $\mathbf{K}$ and $\mathbf{D}_2$ are, respectively, the modal stiffness and damping of the arm links. The model structure (12) holds for any finite dimensional approximation of distributed flexibility, as long as the assumed modes of deformation satisfy the geometric clamped boundary conditions at the base of each link [15]. Accordingly, the input torques $\mathbf{u}$ appear only in the first set of equations. With reference to (1), here $n = 2(N + N_e)$, $m = N$.

For the sake of simplicity, consider the simpler but significative case of deflections limited, for each link, to the plane of rigid motion. Instead of taking cartesian-space quantities, the output can be defined as

$$\mathbf{y} = \theta + \mathbf{C}\delta, \qquad (13)$$

i.e. each component y_i is the rigid joint variable θ_i modified by a linear combination of the variables δ_{ij} associated to link i. Under the hypothesis of small link deformation, $\mathbf{y}$ is one-to-one related to position and orientation of the end-effector through the standard direct kinematics of the arm.

Using (13), the robot dynamics (12) can be rewritten in the new coordinates $(\mathbf{y}, \delta)$:

$$\begin{aligned} &\mathbf{B}_{11}(\mathbf{y}-\mathbf{C}\delta,\delta)\ddot{\mathbf{y}} + \left[\mathbf{B}_{12}(\mathbf{y}-\mathbf{C}\delta,\delta) - \mathbf{B}_{11}(\mathbf{y}-\mathbf{C}\delta,\delta)\mathbf{C}\right]\ddot{\delta} \\ &\qquad + \mathbf{n}_1(\mathbf{y}-\mathbf{C}\delta,\delta,\dot{\mathbf{y}}-\mathbf{C}\dot{\delta},\dot{\delta}) + \mathbf{D}_1(\dot{\mathbf{y}}-\mathbf{C}\dot{\delta}) = \mathbf{u}, \qquad (14a) \\ &\mathbf{B}_{12}^{\mathrm{T}}(\mathbf{y}-\mathbf{C}\delta,\delta)\ddot{\mathbf{y}} + \left[\mathbf{B}_{22}(\mathbf{y}-\mathbf{C}\delta,\delta) - \mathbf{B}_{12}^{\mathrm{T}}(\mathbf{y}-\mathbf{C}\delta,\delta)\mathbf{C}\right]\ddot{\delta} \\ &\qquad + \mathbf{n}_2(\mathbf{y}-\mathbf{C}\delta,\delta,\dot{\mathbf{y}}-\mathbf{C}\dot{\delta},\dot{\delta}) + \mathbf{K}\delta + \mathbf{D}_2\dot{\delta} = \mathbf{0}. \qquad (14b) \end{aligned}$$

The reference state evolution $\mathbf{x}_d$ used in the regulator (3) is equivalently expressed in terms of the new coordinates $\mathbf{y}_d$ and δ_d, and of their derivatives $\dot{\mathbf{y}}_d$ and $\dot{\delta}_d$. By this choice, the problem of finding a solution to (4) reduces to determining only the N_e functions $\delta_d = \pi_\delta(\mathbf{w})$, being $\dot{\delta}_d = \pi_{\dot{\delta}}(\mathbf{w}) = [\partial\pi_\delta/\partial\mathbf{w}]\,\mathbf{s}(\mathbf{w})$ a direct consequence.

Assume that the desired trajectory is generated by a linear exosystem in observable canonical form, so that

$$\mathbf{w}(t) = \{y_{d,i},\ \dot{y}_{d,i},\ \ddot{y}_{d,i},\ \ldots,\ y_{d,i}^{r_i-1};\ i = 1,\ldots,N\} \triangleq \mathbf{Y}_d(t) \qquad (15)$$

can be taken as its state. The reduced solution to (4) is rewritten as $\pi_\delta(\mathbf{Y}_d)$, making explicit that the time evolution of the arm deformation will be a function only of the desired end-effector trajectory and of its time derivatives. Thus, the function π_δ should satisfy equation (14b), evaluated along the nominal output evolution

$$\mathbf{B}_{12}^{\mathrm{T}}(\mathbf{y}_d, \pi_\delta)\ddot{\mathbf{y}}_d + \left[\mathbf{B}_{22}(\mathbf{y}_d, \pi_\delta) - \mathbf{B}_{12}^{\mathrm{T}}(\mathbf{y}_d, \pi_\delta)\mathbf{C}\right]\ddot{\pi}_\delta + \mathbf{n}_2(\mathbf{y}_d, \pi_\delta, \dot{\mathbf{y}}_d, \dot{\pi}_\delta) + \mathbf{K}\pi_\delta + \mathbf{D}_2\dot{\pi}_\delta = \mathbf{0}, \tag{16}$$

where arguments have been indicated in a compact form. It should be stressed that this equation is independent from the applied torque. Being (16) a nonlinear time-varying differential equation, it is hardly impossible to determine a bounded solution in closed-form. Indeed, this would be equivalent to finding proper initial conditions for π_δ and $\dot{\pi}_\delta$ at time $t = 0$ such that forward integration of (16) yields a bounded evolution. A more feasible approach is to approximate the solution of (16), using elements which are bounded functions of their arguments, e.g. making use of polynomials in $\mathbf{Y}_d$. For a second-order expansion, this would lead to an approximation of the form

$$\delta_d = \pi_\delta(\mathbf{Y}_d) = \widehat{\pi}_\delta(\mathbf{Y}_d) + o(\|\mathbf{Y}_d\|^3), \tag{17}$$

with

$$\widehat{\pi}_\delta(\mathbf{Y}_d) = \Pi_1\mathbf{Y}_d + \sum_{i=1}^{N_e}(\mathbf{Y}_d^{\mathrm{T}}\Pi_{2,i}\mathbf{Y}_d)\mathbf{e}_i, \tag{18}$$

where $\mathbf{e}_i$ is the ith column of the identity matrix, and Π_1, $\Pi_{2,i}$ are constant coefficient matrices. As long as each component $y_{d,i}(t)$ of the desired trajectory is bounded together with its derivatives up to the $(r_i - 1)$ order, the approximation $\widehat{\pi}_\delta(\mathbf{Y}_d)$ is necessarily a bounded function of time. The constant coefficients in (18) are determined by plugging this into (16), expanding nonlinear terms up to the second order, and applying the polynomial identity principle. This procedure can be iteratively applied for increasing orders of the polynomial approximation, starting with the linear one. Note that coefficients computed in the kth order expansion are kept also in the following one, resulting in large computational savings: at each step, a linear system of equations has to be solved for the unknown coefficients.

Once this solution is obtained, with any desired order of accuracy, backsubstitution of the reference deformation δ_d, of the desired output trajectory $\mathbf{y}_d$, and of their time derivatives into (14a) will give the nominal feedforward term in the regulation law (3). In fact, $\mathbf{u} = \gamma(\mathbf{Y}_d)$ because $\mathbf{x} = \mathbf{x}_d$ is being assumed. The only approximation involved in this process is the one in (17), while all subsequent steps are consistent. In fact, the obtained feedforward term will keep the whole state evolving along a suitable close approximation to the nominal state reference $\mathbf{x}_d()$.

The above computational procedure corresponds to a direct design of the nonlinear regulator. For the indirect design, the control input $\mathbf{u} = \alpha(\mathbf{x}) + \beta(\mathbf{x})\tilde{\gamma}(\mathbf{w})$ can be recovered again from (14). Under the assumption that $\mathbf{B}_{22} - \mathbf{B}_{12}^{\mathrm{T}}\mathbf{C}$ is nonsingular, acceleration $\ddot{\delta}$ is isolated from (14b) and introduced in (14a). Next, by evaluating $\ddot{\mathbf{y}}$ everywhere as $\ddot{\mathbf{y}}_d$, (14a) will give a nonlinear control law with feedback from the tranformed state $\tilde{\mathbf{x}} = (\mathbf{y}, \delta, \dot{\mathbf{y}}, \dot{\delta})$. The latter is immediately rewritten in terms of the original state $\mathbf{x} = (\theta, \delta, \dot{\theta}, \dot{\delta})$, through (13). Indeed, a further stabilization around $\mathbf{x}_d$ (or

$\tilde{\mathbf{x}}_d$) has to take place. The mixed regulation design is accomplished in a similar way. In this case, the feedback gain will be modulated by part of the inertia matrix.

3. Case Study: A One-Link Flexible Arm

3.1 Dynamic Model

A one-link flexible planar robot arm will be used as a case study for the end-effector tracking problem. For a single link, linear dynamic models are usually assumed when limiting the analysis to small deflections. However, in case of fast motion and/or in presence of heavy carried loads, nonlinear effects arise also in this case due to the larger deformations coming into play. A simple modeling technique divides the flexible link into rigid segments that are connected by elastic springs, where link deformation is concentrated. Following the Lagrangian approach, a nonlinear dynamic model can be obtained in the standard form (12). Explicit expressions that are parametrized in the number of segments have been derived in [8], so that model order can be varied easily to achieve the prescribed accuracy. The following treatment will be limited to the case of two equal segments of uniform mass, moving on the horizontal plane.

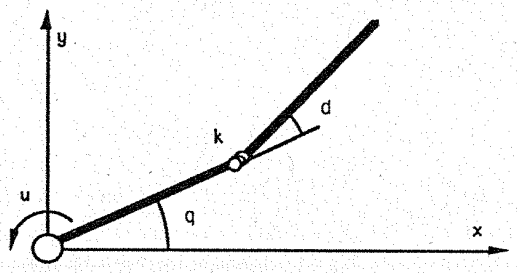

Fig. 4 – A simple one-link flexible arm

Let m and ℓ denote the total link mass and length, and k the spring elasticity. With reference to Fig. 2, θ is the angular position of the joint and δ is the flexible variable, so that $N = N_e = 1$. The dynamic equations are

$$\begin{bmatrix} b_{11}(\delta) & b_{12}(\delta) \\ b_{12}(\delta) & b_{22} \end{bmatrix} \begin{bmatrix} \ddot{\theta} \\ \ddot{\delta} \end{bmatrix} + \begin{bmatrix} n_1(\delta, \dot{\theta}, \dot{\delta}) + d_1\dot{\theta} \\ n_2(\delta, \dot{\theta}) + k\delta + d_2\dot{\delta} \end{bmatrix} = \begin{bmatrix} 1 \\ 0 \end{bmatrix} u, \tag{19}$$

with the elements of the inertia matrix $\mathbf{B}(\delta)$ given by

$$b_{11}(\delta) = a + 2c\cos\delta, \qquad b_{12}(\delta) = b + c\cos\delta, \qquad b_{22} = b,$$

and Coriolis and centrifugal terms

$$n_1(\delta, \dot{\theta}, \dot{\delta}) = -c(\dot{\delta}^2 + 2\dot{\theta}\dot{\delta})\sin\delta, \qquad n_2(\delta, \dot{\theta}) = c\,\dot{\theta}^2 \sin\delta,$$

where $a = 5m\ell^2/24$, $b = m\ell^2/24$, $c = m\ell^2/16$. State equations can be obtained by setting $\mathbf{x} = (\theta, \delta, \dot{\theta}, \dot{\delta}) \in I\!R^4$.

The linearized expression of the end-effector angular position as seen from the base

$$y = \theta + \frac{1}{2}\delta, \tag{20}$$

will be taken as controlled output for the system. The above finite-dimensional model, although of reduced-order, displays the same basic control properties of more accurate and complex distributed models. In particular, (20) is a non-minimum phase output.

3.2 Direct Regulator Design

In order to obtain output tracking of end-effector trajectories for the considered one-link flexible arm, the direct nonlinear regulator design will be followed. Stabilizability of the linear approximation of (19) around the origin $\mathbf{x} = \mathbf{0}$ is easily verified.

An exosystem will be considered, capable of generating polynomial trajectories up to the *fifth order*. In particular, the following linear system of order $r = 6$ in canonical form,

$$\dot{\mathbf{w}} = \begin{bmatrix} 0 & 1 & 0 & 0 & 0 & 0 \\ 0 & 0 & 1 & 0 & 0 & 0 \\ 0 & 0 & 0 & 1 & 0 & 0 \\ 0 & 0 & 0 & 0 & 1 & 0 \\ 0 & 0 & 0 & 0 & 0 & 1 \\ 0 & 0 & 0 & 0 & 0 & 0 \end{bmatrix} \begin{bmatrix} w_1 \\ w_2 \\ w_3 \\ w_4 \\ w_5 \\ w_6 \end{bmatrix} = \mathbf{S}\mathbf{w}, \qquad y_d = w_1 = \mathbf{Q}\mathbf{w}, \tag{21}$$

properly initialized at $\mathbf{w}(0) = (a_0, a_1, 2a_2, 6a_3, 24a_4, 120a_5)$, generates the reference output

$$y_d(t) = a_5 t^5 + a_4 t^4 + a_3 t^3 + a_2 t^2 + a_1 t + a_0. \tag{22}$$

The chain structure of integrators (21) can be extended to the nth order for generating, as y_d, polynomial trajectories of degree $n-1$. Note that, if an infinite time horizon is considered, polynomial trajectories will become unbounded. However, the proper initialization of these exosystems and the limited time span considered in typical robotic applications overcomes this critical point. In the quintic case, different combinations of boundary conditions could be imposed on initial/final position, velocity, acceleration, and jerk. The most practical choice is to set a finite time t_f, with specified initial and final position, velocity and acceleration. For

$$\begin{array}{lll} y_d(0) = y_0 & \dot{y}_d(0) = y_0' & \ddot{y}_d(0) = y_0'' \\ y_d(t_f) = y_f & \dot{y}_d(t_f) = y_f' & \ddot{y}_d(t_f) = y_f'' \end{array} \tag{23}$$

coefficients in (22) take on the values:

$$\begin{bmatrix} a_5 \\ a_4 \\ a_3 \end{bmatrix} = \frac{1}{2t_f^5} \begin{bmatrix} 12(y_f - y_0) - 6t_f(y_f' + y_0') + t_f^2(y_f'' - y_0'') \\ -30t_f(y_f - y_0) + 2t_f^2(7y_f' + 8y_0') - t_f^3(3y_f'' - 2y_0'') \\ 20t_f^2(y_f - y_0) - 4t_f^3(2y_f' + 3y_0') + t_f^4(y_f'' - 3y_0'') \end{bmatrix}, \quad \begin{bmatrix} a_2 \\ a_1 \\ a_0 \end{bmatrix} = \begin{bmatrix} y_0''/2 \\ y_0' \\ y_0 \end{bmatrix}. \tag{24}$$

In order to obtain the reference state trajectory, the general procedure outlined through (14) and (16) will be followed, using the second-order differential representation (18) of the robot system. In particular, (16) becomes

$$(b+c\cos\delta)\ddot{y}_d+(\frac{b-c\cos\delta}{2})\ddot{\delta}+c(\dot{y}_d-\frac{\dot{\delta}}{2})^2\sin\delta+k\delta+d_2\dot{\delta}=0, \tag{25}$$

which should be solved for $\delta(t)=\pi_\delta(\mathbf{Y}_d(t))$. A first-order approximation of this solution will be determined by choosing

$$\begin{aligned}
\delta_d &= \Pi_1\mathbf{Y}_d = p_0y_d+p_1\dot{y}_d+p_2\ddot{y}_d+p_3\dddot{y}_d+p_4y_d^{(4)}+p_5y_d^{(5)},\\
\dot{\delta}_d &= \Pi_1\dot{\mathbf{Y}}_d = p_0\dot{y}_d+p_1\ddot{y}_d+p_2\dddot{y}_d+p_3y_d^{(4)}+p_4y_d^{(5)},\\
\ddot{\delta}_d &= \Pi_1\ddot{\mathbf{Y}}_d = p_0\ddot{y}_d+p_1\dddot{y}_d+p_2y_d^{(4)}+p_3y_d^{(5)}.
\end{aligned} \tag{26}$$

Introducing these formulas for δ, $\dot{\delta}$, $\ddot{\delta}$ into the linearized version of (25) around $\delta=\dot{\delta}=0$,

$$(b+c)\ddot{y}_d+\frac{b-c}{2}\ddot{\delta}+k\delta+d_2\dot{\delta}=0, \tag{27}$$

and solving for the coefficients of y_d and of its derivatives, yields the following explicit expressions:

$$\begin{aligned}
&p_0=0, \qquad p_1=0, \qquad p_2=-\frac{b+c}{k}, \qquad p_3=\frac{d_2(b+c)}{k^2},\\
&p_4=\frac{(b+c)\big((c-b)k+2d_2^2\big)}{2k^3}, \qquad p_5=\frac{d_2(b+c)\big((c-b)k+d_2^2\big)}{k^4}.
\end{aligned} \tag{28}$$

In [8], this kind of approximation was found to leave some steady-state error in the case of a sinusoidal trajectory so that more terms had to be included, at least up to the third order. The second-order approximation (18) simplifies to

$$\delta_d=\Pi_1\mathbf{Y}_d+\mathbf{Y}_d^{\mathrm{T}}\Pi_2\mathbf{Y}_d. \tag{29}$$

Substituting (29) into (25), expanding nonlinear functions and retaining terms up to the second-order, linear terms in the components of $\mathbf{Y}_d$ are matched by the same values (28), while identities on quadratic terms are satisfied by $\Pi_2\equiv\mathbf{0}$. For the third-order approximation

$$\delta_d=\Pi_1\mathbf{Y}_d+\mathbf{Y}_d^{\mathrm{T}}\Pi_2\mathbf{Y}_d+\sum_{\substack{0\le i\le 5\\ k\ge j\ge i}}p_{ijk}\,y_d^{(i)}y_d^{(j)}y_d^{(k)}, \tag{30}$$

(25) should be expanded accordingly as

$$(b+c-\frac{c}{2}\delta^2)\ddot{y}_d+(\frac{b-c}{2}+\frac{c}{4}\delta^2)\ddot{\delta}+c\big(\dot{y}_d-\frac{\dot{\delta}}{2}\big)^2\delta+k\delta+d_2\dot{\delta}=0. \tag{31}$$

Again, using (30) into (31) leads to a linear system of equations for the p_{ijk} unknowns weighting cubic terms in the elements of $\mathbf{Y}_d$. Arising terms of order 4 or more are neglected at this stage. Out of the 56 cubic coefficients, only 34 are non zero: in particular, all coefficients p_{0jk} vanish since deformation cannot depend on y (viz. y_d)

— a cyclic coordinate in the dynamic model (19); furthermore, $p_{111} = 0$ because there are no cubic terms in the velocity $\dot{y}_d$. The rest of the coefficients can be computed numerically, although for this example explicit symbolic expressions in terms of the model parameters were also derived by using *Mathematica*™. Note that most of the cubic coefficients in (30) turn out to be very small numbers, but they multiply high-order derivatives. Thus, simplifications can be carried out only depending on the time scaling of the desired trajectory (i.e. on t_f).

The feedforward term of the direct regulator is obtained using the reference deformation $\delta_d = \delta_d(\mathbf{Y}_d)$ given by (30) in the first equation of the model (19). This provides

$$u = \gamma(\mathbf{Y}_d) = (a + 2c\cos\delta_d)\ddot{y}_d + (b - \frac{a}{2})\ddot{\delta}_d - 2c\dot{y}_d\dot{\delta}_d(\mathbf{Y}_d)\sin\delta_d + d_1(\dot{y}_d - \frac{\dot{\delta}_d}{2}). \quad (32)$$

The feedback action is based on a stabilizing matrix $\mathbf{F}$ (here, a row vector) penalizing the error on the full state $\mathbf{x}$. As a result, the regulator will be

$$u = \gamma(\mathbf{Y}_d) + \mathbf{F}\begin{bmatrix} \theta - (y_d - \delta_d(\mathbf{Y}_d)/2) \\ \delta - \delta_d(\mathbf{Y}_d) \\ \dot{\theta} - (\dot{y}_d - \dot{\delta}_d(\mathbf{Y}_d)/2) \\ \dot{\delta} - \dot{\delta}_d(\mathbf{Y}_d) \end{bmatrix}. \quad (33)$$

3.3 Indirect Regulator Design

Since the relative degree of output (20) is two, the synthesis of an inversion-based control is accomplished by deriving twice the output and setting $\ddot{y} = v$. Solving for u yields

$$\begin{aligned} u &= n_1(\delta, \dot{\theta}, \dot{\delta}) + d_1\dot{\theta} + \frac{b_{11}(\delta) - 2b_{12}(\delta)}{2b_{22} - b_{12}(\delta)}(n_2(\delta, \dot{\theta}) + k\delta + d_2\dot{\delta}) + \frac{2\det B(\delta)}{2b_{22} - b_{12}(\delta)}v \\ &= -c(\dot{\delta}^2 + 2\dot{\theta}\dot{\delta})\sin\delta + d_1\dot{\theta} + \frac{(a - 2b)(c\dot{\theta}^2\sin\delta + k\delta + d_2\dot{\delta}) + 2(ab - b^2 - c^2\cos^2\delta)v}{b - c\cos\delta} \end{aligned} \quad (34)$$

which is in the standard form $u = \alpha(\mathbf{x}) + \beta(\mathbf{x})v$. The input-output linearizing coordinates in the system after inversion are $\tilde{\mathbf{x}} = (y, \dot{y}, \delta, \dot{\delta})$. In view of (20), this implies only a linear transformation in the state space. The closed-loop equations can be written as

$$\begin{aligned} \ddot{y} &= v, \\ \ddot{\delta} &= \frac{2(n_2(\dot{y}, \delta, \dot{\delta}) + k\delta + d_2\dot{\delta})}{b_{12}(\delta) - 2b_{22}} + \frac{2b_{12}(\delta)}{b_{12}(\delta) - 2b_{22}}v, \end{aligned} \quad (35)$$

and it is easy to see that this system is unstable in the first approximation. In particular, this instability is reflected in the system zero-dynamics, which is obtained [8] by imposing $y(t) \equiv 0$ in (35):

$$\ddot{\delta} = -\frac{(c/2)\dot{\delta}^2\sin\delta + 2(k\delta + d_2\dot{\delta})}{b - c\cos\delta}. \quad (36)$$

This confirms that tracking of a desired output trajectory $y_d(t)$ cannot be achieved by simply stabilizing the (linear) input-output behavior in (35), e.g. using

$$v = \ddot{y}_d + \widetilde{F}_1(y - y_d) + \widetilde{F}_2(\dot{y} - \dot{y}_d), \qquad \widetilde{F}_1, \widetilde{F}_2 < 0, \tag{37}$$

as specified in a pure inversion-based approach [16].

As a matter of fact, (34) with (37) will force the state of the system to become unbounded. This is always true, except when the initial arm deformation is exactly in that particular state specified by a bounded solution of the regulator equations, i.e. when $\delta(0) = \delta_d(\mathbf{Y}_d(0))$ and $\dot{\delta}(0) = \dot{\delta}_d(\mathbf{Y}_d(0))$. This instability will be overruled by the linear feedback part in the regulation synthesis of v. The indirect design takes advantage of the simplified structure of system (35). In particular, the reference behavior for the first two states and the feedforward term are in this case

$$\widetilde{\pi}_1(\mathbf{Y}_d) = y_d, \qquad \widetilde{\pi}_2(\mathbf{Y}_d) = \dot{y}_d, \qquad \widetilde{\gamma}(\mathbf{Y}_d) = \ddot{y}_d, \tag{38}$$

i.e. the output reference position, velocity, and acceleration, as expected. On the other hand, references for the deflection variables are the same ones computed for the direct design. The resulting v will be of the form

$$\begin{aligned} v &= \ddot{y}_d + \widetilde{F}_1(y - y_d) + \widetilde{F}_2(\dot{y} - \dot{y}_d) + \widetilde{F}_3(\delta - \delta_d(\mathbf{Y}_d)) + \widetilde{F}_4(\dot{\delta} - \dot{\delta}_d(\mathbf{Y}_d)) \\ &= \ddot{y}_d + \widetilde{\mathbf{F}}(\widetilde{\mathbf{x}} - \widetilde{\mathbf{x}}_d), \end{aligned} \tag{39}$$

which should be compared with (37), as a clear distinction between inversion and regulation. The actual input torque applied to the flexible robot arm is obtained combining (39) with (34).

3.4 Mixed Regulator Design

A mixed regulator can be derived from (34), evaluating nonlinear terms at their desired values but including also the linear stabilization part (39) into v. After some manipulation, the control input becomes

$$u = \gamma(\mathbf{Y}_d) + \frac{2\big(ab - b^2 - c^2\cos^2\delta_d(\mathbf{Y}_d)\big)}{b - c\cos\delta_d(\mathbf{Y}_d)}\,\widetilde{\mathbf{F}}(\widetilde{\mathbf{x}} - \widetilde{\mathbf{x}}_d), \tag{40}$$

where $\gamma(\mathbf{Y}_d)$ is the same as in (32). This expression points out that, in case of matched initial conditions for the full state, the direct regulator (33), the indirect regulator (34) with (37) or (39), and the mixed one (40) all collapse into a unique feedforward law that assigns the same steady-state behavior. However, when initial state matching is impractical, the above control laws will produce different transient errors.

4. Simulation Results

The nonlinear regulator approach has been tested by simulation using as parameters for the one-link flexible arm:

$$\ell = 1\ \text{m}, \quad m = 0.2\ \text{kg}, \quad k = 5\ \text{Nm/rad}, \quad d_1 = d_2 = 0.01\ \text{Nmsec/rad}. \tag{41}$$

Simulations were run using *Matlab*™, with a fourth order Runge-Kutta integration method. For the quintic polynomial trajectory, the following data were used:

$$y_0 = 0°, \quad y_f = 90°, \quad y_0' = y_f' = y_0'' = y_f'' = 0, \quad t_f = 1 \text{ sec.} \tag{42}$$

After t_f, the reference state is forced to zero, except for $y_d = \theta_d = 90°$. This corresponds to reset instantaneously the exosystem state, a critical operation that will cause disturbance on tracking. The feedback gain matrix $\widetilde{\mathbf{F}}$ of the indirect design was chosen by assigning poles at $-20 \pm i30$ and $-30 \pm i25$ to the linearized system. In all other cases, gains were determined in a consistent way so to allow a significative comparison.

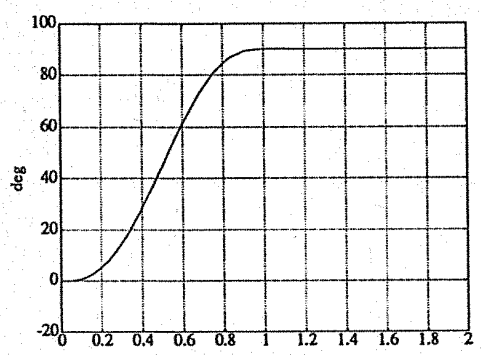

Fig. 5 – Output for a quintic polynomial

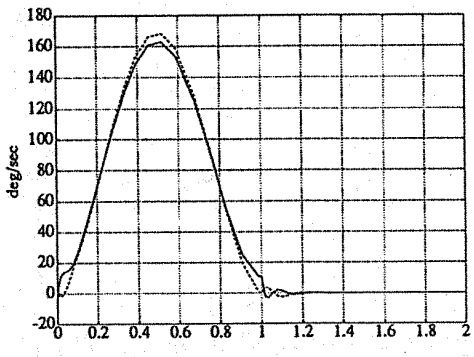

Fig. 6 – Joint and tip velocity

Figures 5–8 show the obtained tracking results for the quintic polynomial case using the indirect regulator law (34) with (39). The desired and the obtained output are practically coincident, even in the presence of a peak velocity reaching more than 160°/sec at the trajectory midpoint. As shown in Fig. 6, the velocity of the joint (continuous line) and that of the tip (dashed) are slightly different in magnitude. The non-minimum phase nature of the system is displayed in the reverse initial motion of the tip. A more detailed view of the tracking error $e = y - y_d$ is given in Fig. 7. The maximum error value is about 0.15° and vanishes in 0.2 sec: from there on, exact tracking follows. The presence of a transient error at $t_f = 1$ sec is a consequence of the exosystem reset which produces a mismatch with the current state of the flexible arm. The input torque u in Fig. 8 is similar to the one necessary for an equivalent rigid arm — a cubic as the desired acceleration profile. Differences arise at the beginning and at the end of the motion, in response to state errors. Note that no excess torque is required for the flexible case. When applying the direct regulator design (33), which uses pure linear feedback and feedforward based on the nonlinear model, no relevant differences were found.

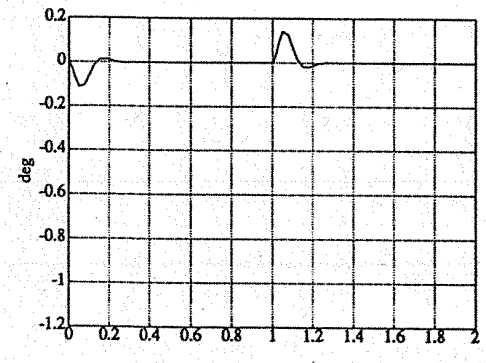

Fig. 7 – Error for a quintic polynomial

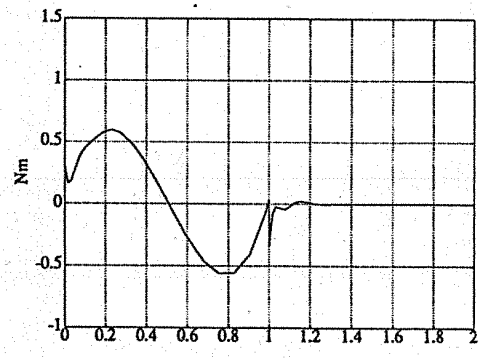

Fig. 8 – Torque for a quintic polynomial

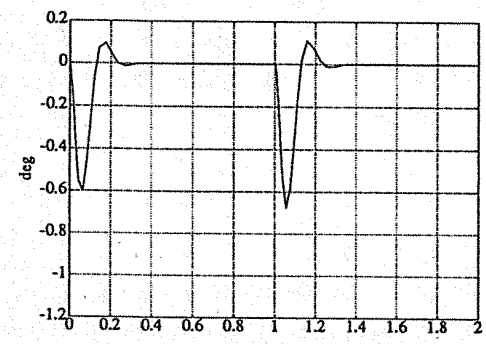

Fig. 9 – Error for a cubic polynomial

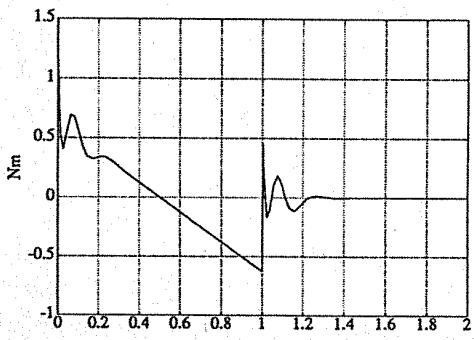

Fig. 10 – Torque for a cubic polynomial

In order to assess the effect of trajectory smoothness, the same net motion was accomplished using a cubic polynomial with zero initial and final velocity. Tracking error and required torque are shown respectively in Fig. 9 and 10. The maximum error is about six times higher, but still very small. Non-zero torques at the initial and final instants correspond to step changes in the desired acceleration, with an added peak due to transients. Moreover, the quintic polynomial trajectory roughly halves the deflection δ and its time derivative (Fig. 11) with respect to the cubic case. Note that, for this very smooth trajectory, the maximum deflection is about 2.5°.

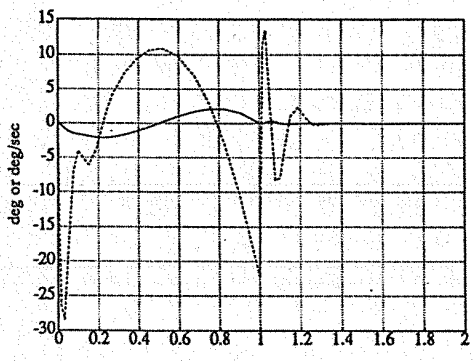

Fig. 11 – Flexible variables

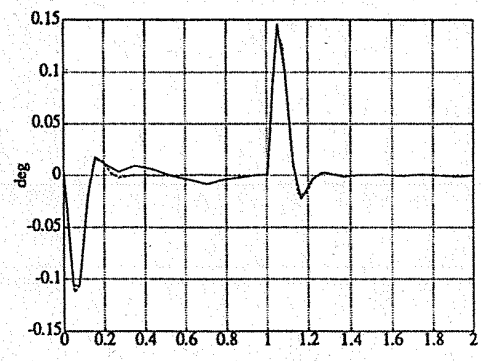

Fig. 12 – Linear vs. nonlinear regulation error

It is also interesting to compare the performance of the nonlinear regulator with respect to a linear one, i.e. using (8) designed on the linearized system. Figure 12 shows a very similar error behavior in the linear (continuous line) and in the nonlinear (dashed) case. This is not unexpected because of the very small nonlinearities coming into play. However, while peak transient errors are identical, the remaining behavior during motion (between 0.2 and 1 sec) is qualitatively different, giving perfect tracking only for the nonlinear regulator. This becomes also more apparent when considering the case of fast sinusoids, as reported in [8].

The performance of the mixed regulator design (40) is also quite satisfactory, as shown in Figs. 13–14 for the quintic polynomial. An initial position error of about 9° was assumed in this case, so to emphasize closed-loop convergence of state trajectories towards the reference one. In particular, Fig. 14 indicates a rapid and well damped transient according to the chosen pole location of the linear feedback. The small error appearing after t_f is the same as in Fig. 7, shown with a different scale.

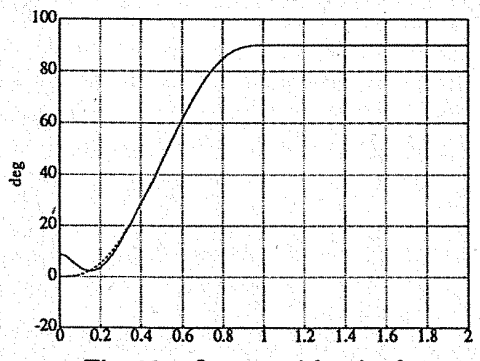

Fig. 13 – Output with mixed regulator design

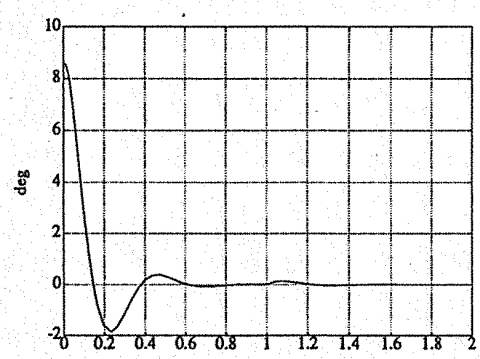

Fig. 14 – Error with mixed regulator design

5. Conclusions

Nonlinear control theory offers several techniques to deal with the problem of tracking trajectories for robot arms with flexible links. In particular, the regulation approach is well suited in the case of end-effector tracking, as it is a natural framework for solving the closed-loop instability phenomena arising with standard inversion techniques. It has been pointed out that, for flexible manipulators, solving the regulator equations accounts in determining the nominal deformation associated with the desired output motion. This allows to set up an efficient computational procedure for deriving the regulation control law.

Different possible realizations of nonlinear regulators have been presented, highlighting tracking capabilities and ease of implementation. Simulation results have shown that tracking can be quite accurate when smooth reference trajectories are selected. Work is under way for extending the application of this control strategy to multi-mode/multi-link flexible robot arms. The proposed feedforward/feedback schemes will be evaluated in the experimental test bed available in our Robotics Laboratory [17].

Finally, it is worth to remark that the conditions under which a nonlinear regulator can be successfully designed using static state-feedback are the same which allow regulation using only output measurements, provided that a reasonable observability hypothesis is satisfied and that dynamics is included in the controller. Conversely, the stabilizability of the nonlinear system, which is needed for regulation, does not necessarily ask for full state feedback. For instance, feedback from the flexible variables may be avoided. Further investigation is being devoted to these aspects.

Acknowledgements

This paper is based on work supported by the *Ministero dell'Università e della Ricerca Scientifica e Tecnologica* under 40% funds (Scientific Director: Prof. F. Nicolò).

References

[1] W.J. Book, "Modeling, design, and control of flexible manipulators arms: A tutorial review," *29th IEEE Conf. on Decision and Control* (Honolulu, HI, Dec. 5–7, 1990), pp. 500–506.

[2] M.J. Balas, "Fedback control of flexible systems", *IEEE Trans. on Automatic Control*, vol. AC-23, no. 4, pp. 673–679, 1978.

[3] B. Siciliano and W.J. Book, "A singular perturbation approach to control of lightweight flexible manipulators," *Int. J. of Robotics Research*, vol. 7, no. 4, pp. 79–90, 1988.

[4] S.N. Singh and A.A. Schy, "Control of elastic robotic systems by nonlinear inversion and modal damping," *ASME J. of Dynamic Systems, Measurements, and Control* vol. 108, no. 5, pp. 180–189, 1986.

[5] A. De Luca, P. Lucibello, and G. Ulivi, "Inversion techniques for trajectory control of flexible robot arms," *J. of Robotic Systems*, vol. 6, no. 4, pp. 325–344, 1989.

[6] R.H. Cannon, Jr. and E. Schmitz, "Initial experiments on the end-point control of a flexible one-link robot," *Int. J. of Robotics Research*, vol. 3, no. 3, pp. 62–75, 1984.

[7] C. Byrnes and A. Isidori, "Local stabilization of critically minimum phase nonlinear systems," *Systems and Control Lett.*, vol. 11, no. 1, pp. 9–17, 1988.

[8] A. De Luca, L. Lanari, and G. Ulivi, "Output regulation of a flexible robot arm," *9th INRIA Int. Conf. on Analysis and Optimization of Systems* (Antibes, F, Jun. 12–15, 1990), pp. 833–842.

[9] A. De Luca, L. Lanari, and G. Ulivi, "Nonlinear regulation of end-effector motion for a flexible robot arm," *Joint Conf. on New Trends in Systems Theory* (Genova, I, Jul. 9–11, 1990).

[10] E. Bayo, "A finite-element approach to control the end-point motion of a single-link flexible robot," *J. of Robotic Systems*, vol. 4, no. 1, pp. 63–75, 1985.

[11] M. Poloni and G. Ulivi, "Iterative trajectory tracking for flexible arms with approximate models," *5th Int. Conf. on Advanced Robotics (ICAR'91)* (Pisa, I, Jun. 20–22, 1991).

[12] T. Kokkinis and M. Sahraian, "Flexible robot arm control: An optimal solution for the inverse dynamics," *IEEE Work. on Intelligent Motion Control* (Istanbul, TR, Aug. 20–22, 1990), pp. 529–534.

[13] A. Isidori and C. Byrnes, "Output regulation of nonlinear systems," *IEEE Trans. on Automatic Control*, vol. AC-35, no. 2, pp. 131–140, 1990.

[14] A. Isidori, *Nonlinear Control Systems*, 2nd Edition, Springer Verlag, Berlin, 1989.

[15] L. Meirovitch, *Analytical Methods in Vibrations*, Macmillan, New York, 1967.

[16] R.M. Hirschorn, "Output tracking in multivariable nonlinear systems," *IEEE Trans. on Automatic Control*, vol. AC-26, no. 2, pp. 593–595, 1981.

[17] A. De Luca, L. Lanari, P. Lucibello, S. Panzieri, and G. Ulivi, "Control experiments on a two-link robot with a flexible forearm," *29th IEEE Conf. on Decision and Control* (Honolulu, HI, Dec. 5–7, 1990), pp. 520–527.